Theoret. Comput. Fluid Dynamics (1998) 11: 263–279

Theoretical and Computational Fluid Dynamics

Stratified Atmospheric Boundary Layers and Breakdown of Models[1]

L. Mahrt[2]
National Center for Atmospheric Research,
Boulder, CO 80307, U.S.A.

Communicated by J.R. Herring

Received 13 June 1997 and accepted 19 November 1997

Abstract. The goal of this study is to assess complications in atmospheric stable boundary layers which are not included in numerical models of the stably stratified boundary layer and to provide a formulation of surface fluxes for use in numerical models. Based on an extensive interpretive literature survey and new eddy correlation data for the stable boundary layer, this study defines two prototype stable boundary layers: the weakly stable case and the very stable case. The weakly stable boundary layer is amenable to existing models. The very stable boundary layer eludes modeling attempts due to breakdown of existing formulations of turbulence and due to features found in the atmosphere which are not normally included in models. The latter includes clear-air radiative cooling, low-level jets, surface heterogeneity, gravity waves, meandering motions, and other mesoscale motions which propagate from outside the local domain. While these mechanisms are not essential to understanding idealized or laboratory versions of the stable boundary layer, they complicate comparisons of numerical models and theories with actual atmospheric boundary layers. Statistics which describe various features of the stable boundary layer are offered for future comparison with modeling results.

1. Introduction

Examination of stratified turbulence in atmospheric boundary layers is complicated by a multiplicity of physical influences including clear-air radiative flux divergence, elevated shear associated with low-level jets, increased relative importance of meandering motions, gravity waves, and increased relative importance of surface heterogeneity and local slopes. Some or all of these mechanisms may be absent in modeling studies. To examine the various complexities of the stable boundary layer, it will be useful to define two prototype stable boundary layers: the *very stable boundary layer* and the *weakly stable boundary layer*, as sketched in Figure 1. Such a classification will help organize our discussions even though such a classification is over-simplified and most stable boundary layers lie somewhere between these two idealized states.

The weakly stratified boundary layer over land is normally characterized by windy conditions and/or cloudy conditions such that the surface cooling is relatively slow. In contrast, the very stable boundary layer is characterized by weak winds and clear skies, corresponding to strong net radiative cooling at the surface. Little is known about the very stable boundary layer even though this is of considerable practical importance.

[1] Part of this work was carried out while a visitor at the European Centre for Medium Range Forecasting, Reading, Berkshire RG2 9AX, England. This material is based upon work supported by Grant DAAH04-96-10037 from the U. S. Army Research Office and Grant ATM-9310576 from the Physical Meteorology Program of the National Science Foundation.

[2] On leave from the College of Oceanic and Atmospheric Sciences, Oregon State University, Corvallis, OR 97331, U.S.A.

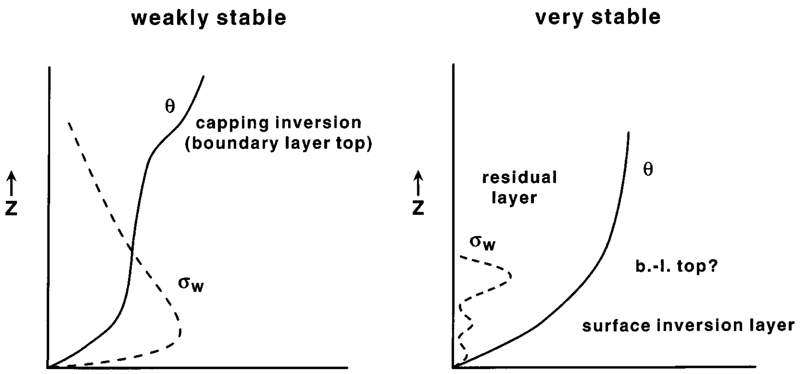

Figure 1. Idealized schematic contrasting the vertical structure of the weakly stable and very stable boundary layers. σ_w is the standard deviation of the vertical velocity fluctuations and θ is the potential temperature, analogous to density in an incompressible fluid.

The turbulence in this case is weak and intermittent allowing buildup of large near-surface concentrations of contaminants. Because the downward turbulent heat flux is limited for this case, strong surface cooling may correspond to unusually cold temperatures and frost damage.

Most of our knowledge and modeling capability for the stable boundary layer is confined to the weakly stable boundary layer and it is not clear if present modeling capability can approximate any of the main features of the very stable boundary layer. Formulations of turbulence for the very stable case is limited by the fact that measurement of covariances and higher-order statistics in weak and intermittent turbulence requires an averaging time that is so long that nonstationarity of the mean flow is inadvertently captured (Wyngaard, 1973).

While we normally associate stably stratified boundary layers in the atmosphere with nocturnal conditions, stable boundary layers are generated by a variety of other mechanisms including advection of warm air over a cold surface. The usual nocturnal boundary layer is generated by net radiative cooling at the surface. The surface cools the adjacent air through thermal conduction in the molecular sublayer and ultimately through downward turbulent transfer of heat from the air above the molecular sublayer. In the atmosphere, the Reynolds number is large and the molecular sublayer is usually thin (a few millimeters) compared with the thickness of the stable boundary layer (typically 50–500 m).

The following provides an overview of the qualitative nature of stable atmospheric boundary layers and introduces a number of features (Sections 4–5) which are probably not known to most fluid dynamicists and in any event not included in numerical models of the stable boundary layer. The subject area is fascinating and elusive in that our concepts of stratified turbulence based on theory and laboratory results are difficult to verify in actual stratified atmospheric boundary layers. At the risk of confusing the overall picture, the following interpretation of the existing literature includes studies which seem to contradict the main view. The picture is partially clarified by appealing to new eddy correlation data collected in the stable atmospheric boundary. These data were collected over simple, relatively flat, grassland in Kansas during March 1995 in the Microfronts project. Eddy correlation data for computing fluxes of momentum, heat and moisture were collected at 3 m and 10 m and detailed profiles were measured in the lowest 10 m. These data were described in more detail in Sun (1997). The data set is particularly useful since it includes fluxes at two levels and includes a wide range of stability.

In the next section we review the usual formulation of surface fluxes and then provide a self-contained formulation of surface fluxes for use in numerical models of the stable boundary layer. In the subsequent section the bulk structure of the stable boundary layer is examined.

2. Surface Fluxes

A critical part of modeling the stably stratified boundary layer is formulating the surface fluxes. The surface buoyancy flux and stress along with the mean stratification determine the basic characteristics of the stable boundary layer. No matter how sophisticated the numerical simulation, the surface fluxes must be parametrized or specified independently as boundary conditions. Specification of the surface fluxes independently of the model removes important coupling between the surface and the stable boundary layer.

Surface fluxes are normally formulated in terms of the bulk aerodynamic formula using the mean wind speed at the first model level. For heat and momentum, these formulations are written as

$$\begin{aligned}\overline{w'\theta'} &= C_{\mathrm{H}}\overline{u}[\theta_o - \theta(z)],\\ \overline{w'u'} &= C_{\mathrm{D}}\overline{u}^2,\end{aligned} \tag{1}$$

where C_{H}, is the transfer coefficient for heat, C_{D} is the surface drag coefficient, z is the first model level or observational height, θ_0 is the aerodynamic surface temperature (discussed below), and $\overline{u}$ is the speed of the vector-averaged wind where the coordinate system has been rotated in the direction of the mean wind. Here we have assumed that the surface stress is aligned with the surface wind, as implicitly assumed in Monin–Obukhov similarity theory. While such an assumption may not always be a good approximation, more general formulations are not available.

Using Monin–Obukhov similarity theory, the drag coefficient and transfer coefficient for heat are estimated as

$$\begin{aligned}C_{\mathrm{H}} &= \left[\frac{k}{\ln(z/z_0) - \psi_m}\right]\left[\frac{k}{\ln(z/z_{0T}) - \psi_{\mathrm{h}}}\right]\\ C_{\mathrm{D}} &= \left[\frac{k}{\ln(z/z_0) - \psi_m}\right]^2\end{aligned} \tag{2}$$

where z_0 and z_{0T} are the roughness lengths for momentum and heat, respectively, and ψ_{m} and ψ_{h} are the stability functions for momentum and heat, respectively (Section 2.1). These functions are historically determined by first fitting the nondimensional profile functions

$$\varphi_{\mathrm{h}}\left(\frac{z}{L}\right) \equiv -\frac{(\partial\overline{\theta}/\partial z)(kzu_*)}{\overline{w'\theta'}(z)}, \tag{3}$$

$$\varphi_{\mathrm{m}}\left(\frac{z}{L}\right) \equiv \frac{(\partial\overline{u}/\partial z)(kz)}{u_*}, \tag{4}$$

$$L \equiv -\frac{u_*^3}{\kappa(g/\theta)\overline{w'\theta'}} \tag{5}$$

to dependencies on z/L where L is the Obukhov length, $u_* \equiv \overline{w'u'}^{1/2}$ is the surface friction velocity, and κ is the von Karmen constant, typically taken to be about 0.4. These relationships are valid in the surface layer above the roughness sublayer (Figure 2). The roughness sublayer is the region adjacent to the surface where the wakes of individual roughness elements influence the time-averaged flow. That is, the time-averaged flow in the roughness sublayer varies horizontally according to position with respect to individual roughness elements. The surface layer is assumed to be sufficiently thin that the variation of fluxes across the surface layer can be neglected; that is, the fluxes are assumed to be constant. At higher levels, where the fluxes are significantly different from the surface fluxes and the height-dependence of the fluxes cannot be neglected, the above relationships are sometimes framed in terms of *local similarity theory* (Nieuwstadt, 1984) where the surface values of the fluxes are replaced by their local height-dependent values (Figure 2).

The nondimensional profile functions $\varphi_{\mathrm{h}}(z/L)$ and $\varphi_{\mathrm{m}}(z/L)$ are vertically integrated to obtain ψ_{h} and ψ_{m} which are required to evaluate the transfer coefficient (equation (3)). This vertical integration requires that the fluxes and the wind direction are approximately height-independent.

To close the problem, one must specify the roughness lengths for heat and momentum and determine a method for estimating the surface aerodynamic temperature. The problem becomes easily confused in the literature, particularly in studies which reconsider the form of the stability functions. Formally, the aerodynamic temperature corresponds to the temperature extrapolated downward to the surface roughness height using (3). Since Monin–Obukhov similarity theory is not valid in the roughness sublayer immediately adjacent to the surface, the required aerodynamic temperature can not be systematically identified with any observable surface temperature.

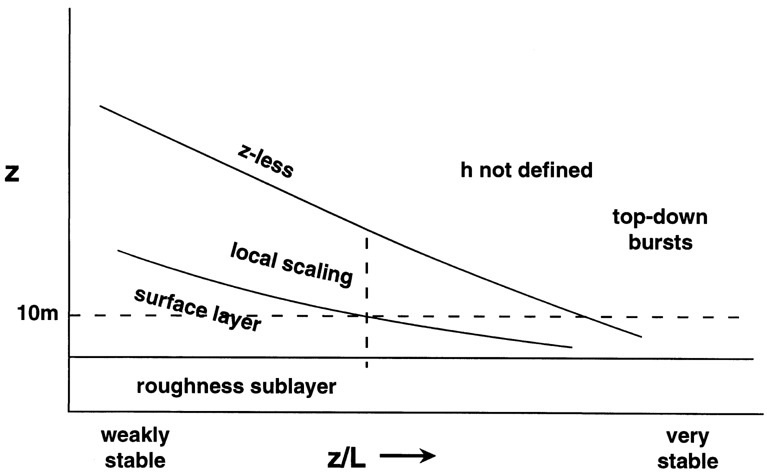

Figure 2. Different stable boundary-layer regimes as a function of stability. The vertical dashed line indicates the value of z/L corresponding to maximum downward heat flux.

In practice, the aerodynamic temperature is replaced with the temperature of the solid surface. In models, the surface temperature can be computed from the surface energy balance or externally specified as a boundary condition. Use of the surface temperature in place of the aerodynamic temperature *redefines* the roughness length for heat which is then computed from data using Eqs. 2 and 3, the observed fluxes and the specified stability functions $\varphi_{\mathrm{h}}(z/L)$ and $\varphi_{\mathrm{m}}(z/L)$.

The thermal roughness length is usually specified to be less than the momentum roughness length although observations over a variety of surfaces collectively suggest that the thermal roughness is not closely related to the momentum roughness length and is sometimes erratic and unpredictable (see Sun and Mahrt (1995); and papers surveyed in Mahrt (1996)). Unfortunately, calculations of z_{0T} from observations in the stable atmospheric boundary layer are almost nonexistent. Sun (1997) finds that in the stable boundary layer over a simple grass surface, z_{0T} is uncorrelated with z_0 but is generally smaller than z_0 and sometimes reaches extremely small values. The erratic behavior of z_{0T} probably indicates that applying Monin–Obukhov similarity to compute the heat flux using a single surface temperature is flawed. Certainly, over complicated surfaces, multiple surface temperatures are required and the use of a single surface temperature is inadequate. This topic is beyond the scope of this review.

The erratic behavior of the thermal roughness length led Mahrt *et al.* (1997a) and Sun *et al.* (1997) to eliminate the thermal roughness length as an unknown by equating it with the momentum roughness length. This defines the surface aerodynamic temperature which must then be related to practical observable temperatures. The problem has not been closed in a general way.

In the following, we proceed with the usual replacement of the aerodynamic temperature with the temperature of the surface and return to the early practice of equating the thermal roughness length to the momentum roughness length:

$$z_{0T} = z_0. \tag{6}$$

The philosophy is to be as simple as possible until more sophisticated formulations can be fully justified. This is the approach followed below. Using (6) and the value of the surface temperature for the surface aerodynamic temperature, the heat flux can be predicted from (2)–(3), provided that the stability functions ψ_{h} and ψ_{m} are known.

2.1. Stability Functions

The usual route for estimating the stability functions is first to determine the dependence of the nondimensional profile functions $\varphi_{\mathrm{h}}(z/L)$ and $\varphi_{\mathrm{m}}(z/L)$ and then to integrate them vertically. The advantage of determining $\varphi_{\mathrm{h}}(z/L)$ and $\varphi_{\mathrm{m}}(z/L)$ is that they are calculated from data in the surface layer independently of surface properties and values of the roughness lengths. However, estimation of $\varphi_h(z/L)$ and $\varphi_m(z/L)$ require detailed wind and temperature profiles.

The nondimensional profile functions for heat and momentum for stable conditions are often parametrized in terms of the "log-linear" form (Zilitinkevich and Chalikov, 1968; Businger *et al.*, 1971; Yaglom, 1977)

$$\varphi_h = 1 + \frac{\beta z}{L}, \tag{7}$$

$$\varphi_m = 1 + \frac{\alpha z}{L} \tag{8}$$

where α is generally specified to be equal to, or greater than, β for stable stratification where the latter condition corresponds to a Prandtl number greater than unity.

The log-linear form of the profile functions (7)–(8) can be integrated to obtain relatively simple forms of the stability functions. The stability functions presented in Businger *et al.* (1971), sometimes known as the Businger–Dyer relationships, are of the form

$$\psi_h = \psi_m = -\frac{\gamma z}{L} \tag{9}$$

where γ is typically chosen to be 5. However, the validity of (7) and (8), and therefore (9), has been challenged in numerous studies for the very stable case.

For the very stable case, three possibilities must be considered:

1. The log-linear law remains valid for the very stable case (Section 2.2).
2. Monin–Obukhov similarity theory is valid but the log-linear form of the stability function is not valid (Section 2.3).
3. Monin–Obukhov similarity theory is not valid due to effects not included in the stability parameter z/L (Section 2.4).

2.2. Log-Linear Law and z-Less Stratification

First consider the behavior of the log-linear law for heat in the very stable case. In the limit when $\beta z/L$ in (8) becomes large compared with unity, we note, from the definition of φ_h, that z cancels on both sides of the equation in which case

$$\frac{\kappa\, \partial\theta/\partial z}{\theta_*} = \frac{\beta}{L}. \tag{10}$$

Substitution for the expressions for L and θ_* yields a relationship for the heat flux and the vertical gradient of potential temperature which is independent of z. This is a special case of "z-less" stratification (Wyngaard, 1973; Hicks, 1976; Nieuwstadt, 1984; Dias *et al.*, 1995). The concept of z-less stratification occurs when the turbulence is sufficiently constrained by buoyancy; that is, not directly influenced by the ground surface. Then height above the ground is not a scaling parameter and local scaling is valid. This condition is thought to describe the interior of the stable boundary layer with sufficient stratification. In the very stable case, z-less stratification may extend closer to the ground surface as sketched in Figure 2 and predicted by (10).

2.3. Alternate Stability Functions

However, some observational studies suggest that the log-linear law is not valid for the very stable case. As a rough estimate, Taylor (1971) suggests that the log-linear similarity theory breaks down for $z/L > \frac{1}{2}$. Although the general arguments in Taylor (1971) were questioned by Arya (1972), the specific prediction of breakdown of the log-linear law is also supported by the observations of Hicks (1976). Mahli (1995) similarly finds that the log-linear law breaks down for $z/L > 1$. Holtslag (1984) concludes that prediction of surface fluxes in the stable boundary layer for winds less than 1 m/s (presumably very stable) is usually problematic.

Modified formulations have been suggested by Webb (1970), Hicks (1976), Kondo *et al.* (1978), Louis (1979), Holtslag (1984), Holtslag and De Bruin (1988), Beljaars and Holtslag (1991), and Launiainen (1995), although some of these studies inferred the stability functions from profiles alone without actual eddy correlation data. A review of the stability functions are presented in Högström (1988, 1996). The modified forms generally restrict the increase of φ_{h} with increasing z/L for very stable conditions (large z/L). This modification corresponds to greater heat flux for a given vertical temperature gradient and stability.

Howell and Sun (1997) compute fluxes from the Microfronts data using a variable averaging length which is dependent on the flow itself. They find that the stability function for momentum lies numerically between those of Businger *et al.* (1971) and Beljaars and Holtslag (1991). They find that the heat flux and the stability function for heat, ψ_{h}, are sensitive to the choice of observational height even in the lowest 10 m.

In contrast to the above studies, Sethuraman and Brown (1976) find that the log-linear form is valid for z/L much larger than one. They attributed this behavior to the large roughness of the surface. Since the stability functions are assumed to be independent of the roughness length, the arguments of Sethuramen and Brown (1976) contradict Monin–Obukhov similarity theory.

However, most studies suggest that the log-linear law underestimates the surface flux for very stable conditions. In numerical models, the underestimated downward heat transport leads to unrealistic surface cooling. This cooling further stabilizes the boundary layer which in turn further reduces the turbulence and downward heat flux. The final result may be total collapse of the turbulence and "run-away" surface cooling due to the uncompensated surface radiative heat loss. This cooling eventually leads to radiative equilibrium between the surface and the atmosphere which corresponds to unrealistically low surface temperatures.

2.4. Additional Length Scales

The uncertainty of the form of the stability functions φ_{m} and φ_{h} for very stable conditions could be due to the difficulty of measuring fluxes under such conditions or may be an inadvertent attempt to compensate for additional affects not included in Monin–Obukhov similarity theory. Smedman *et al.* (1993) concludes that conditions for surface layer similarity theory are not met when the principal source of turbulence is aloft as might occur with significant shear associated with a low-level jet. Intermittent downward transport of heat by shear-generated turbulence above the surface-based nocturnal inversion has been observed by Mahrt (1985), Smedman (1988), and Nappo (1991). Then the conditions for Monin–Obukhov similarity theory may not be met in that this downward transport probably does not scale with the Obukhov length. Modification of the nondimensional profile functions in Section 2.3 might be due to an attempt to compensate statistically for sources of heat flux not included in Monin–Obukhov similarity theory.

However, in contrast to the above studies which suggest that φ_{h} is smaller (greater heat flux) than predicted by the log-linear law, Smedman *et al.* (1995) found that the φ functions were much larger than predicted by Monin-Obukhov similarity theory for stable offshore flows in the presence of a low-level jet. This implies that for a given vertical gradient, fluxes are weaker in the presence of a low level jet. On the other hand, the nondimensional velocity and temperature gradients obeyed Monin–Obukhov similarity at the same location for stable cases without a jet (Bergström and Smedman, 1995). Smedman *et al.* (1995) also observed that larger eddies were suppressed by the low-level jet which is thought to be responsible for the reduced transport. These data sets were characterized by $z/L < 1$ and therefore did not represent the very stable case. In a similar study, Mahrt *et al.* (1997b) also found that existing similarity theories overestimate the surface heat flux in stable offshore flows. They listed a number of possible causes including suppression of large transporting eddies by the low top of the internal boundary layer. However, they were unable to isolate a specific mechanism as the main cause.

The above studies suggest that the flux–gradient relationship at z, the first model level or observational level, may be influenced by additional length scales such as the boundary-layer depth or height of the low-level jet. Alternatively, the surface layer, where the flux-gradient relationship is influenced by only z/L, may be confined to a layer below the level z.

From another point of view, the flux decreases significantly between the surface and the level z when z/L is large. In the stable atmospheric boundary layer, Högstöm (1988) observed a decrease of flux with height even within the lowest 10 m. Even with modest stability in the classical Kansas experiment, the heat flux decreased by typically 20% between the 6 m and 23 m levels (see Figure 10 of Haugen *et al.* 1971). Substantial vertical divergence of the heat flux is observed in the lowest 10 m in Howell and Sun (1997). The divergence may be larger than inferred from the data since the flux at the lowest level could be underestimated with standard sonic anemometers where transport by small eddies close to the ground is not completely captured due to pathlength averaging of the instrument.

A substantial decrease of the flux between the surface and level z implies that the flux is influenced by the depth of the boundary layer, that is the depth where the flux vanishes. Then z/L alone is inadequate to predict the flux at level z. Perhaps choosing a lower value of z (higher model resolution or attempting to measure fluxes closer to the surface) would improve the applicability of Monin–Obukhov similarity theory.

We summarize the above results by suggesting that when z/L is larger than unity, the existing calibration of the φ functions is uncertain. When z/h is not small compared with unity, flux divergence between the surface and level z may invalidate application of Monin–Obukhov similarity theory. The latter breakdown may be more severe with the occurrence of low-levels jets. However, such conclusions are partly speculation and more observations are needed.

2.5. Final Recommendation for Surface Fluxes

The above subsections show that existing surface formulations are not trustworthy in the very stable case. Existing surface flux formulations may also be invalidated with low-level jets, sloped surfaces, surface hete-orogeneity and significant clear-air radiative flux divergence. With these serious warnings in mind, the bulk aerodynamic formula is recommended with the thermal roughness length simply equated to the momentum roughness length (equation 6) and the stability functions simply estimated from (9). The formulation of the thermal roughness length is the most tenuous part of the package but more sophisticated formulations cannot be justified based on existing data. Considering the new evidence and formulations for the very stable case surveyed in the above section, these conservative recommendations might seem like a step backwards in time. The philosophy adopted here is that newer more sophisticated formulations are still characterized by large uncertainty and the increased complexity is not justified. From an observational point of view, real progress will not be made until field work with improved instrumentation is dedicated to the very stable boundary layer. However, this is beyond the scope of this paper.

3. Bulk Structure

Based on observations of stable atmospheric boundary layers, this section describes the vertical structure above the surface layer in the so-called “outer layer” of the boundary layer.

3.1. Weakly Stable

In the *weakly stable boundary layer*, the turbulence is more continuous in time and space and is more likely described by existing similarity theory in both the outer layer and in the surface layer. The weakly stable boundary layer is the usual “textbook” nocturnal boundary layer and has been examined with (a) atmospheric observational studies (e.g., Lenschow *et al.* 1988a,b), theoretical studies (e.g., Derbyshire, 1990), and (c) similarity theories (e.g., Zilitinkevich and Mironov, 1996). Almost all modeling studies (e.g., Brost and Wyngaard, 1978) as well as recent large-eddy simulations (LES) of the nocturnal boundary layer (Mason and Derbyshire, 1990; Brown *et al.* 1994; Andrén, 1995) have concentrated on the weakly stable case.

The weakly stable case can be defined in terms of the stability of the surface layer, z/L. For weak stratification (small z/L), the magnitude of the downward heat flux is limited by the smallness of the temperature stratification and vanishes as the temperature stratification vanishes (neutral stratification). With stronger stratification, the downward heat flux becomes limited by the buoyancy constraints on the turbulence and vanishes as the stratification becomes sufficiently large to suppress the turbulence completely. Between these two regimes, maximum downward heat flux occurs (Figure 2). Mahli (1995) finds the maximum downward heat flux occurs at z/L = 0.2. For the Microfronts data, the maximum heat flux occurs at roughly

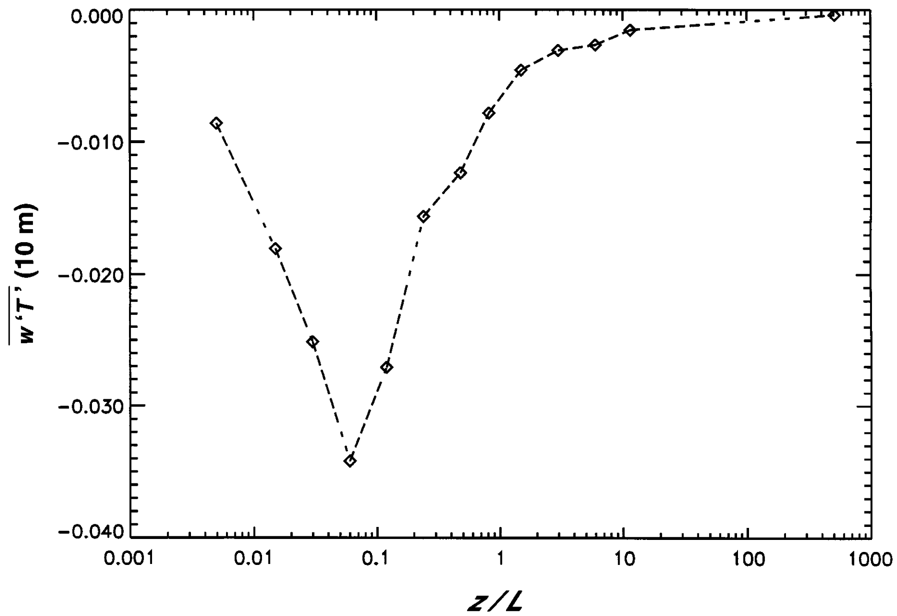

Figure 3. The heat flux as a function of stability for the Microfronts data.

z/L = 0.05 for 10 m data (Figure 3) but depends on the measurement height. In either study, the maximum downward heat flux occurs at values of z/L which are smaller than the order of one value thought to mark the beginning of the breakdown of the log-linear law which here defines the beginning of the very stable regime.

Between the stable surface layer and inversion layer capping the weakly stratified boundary layer, the profile of potential temperature may be nearly well mixed (Figure 1) corresponding to an inflection point in the flow profile (Van Ulden and Wieringa, 1996). Otte and Wyngaard (1996) apply a series expansion to the basic equations where the zero-order state is the well-mixed layer and corrections to this state are higher-order terms. However, even for the weakly stratified partially mixed layer, shear production of turbulence energy is important in the upper part of the boundary layer (Vogelezang and Holtslag, 1996).

In contrast to the very stable case, the depth of the boundary layer seems definable in the weakly stratified case. In some models the boundary-layer depth is explicitly modeled, while in other models the boundary-layer depth is not needed or is diagnostically computed from the predicted vertical distribution of turbulence kinetic energy. Zilitinkevich and Mironov (1996) provide a comprehensive survey of different models of the stable boundary-layer depth. They organize their comparisons in terms of the vertically-integrated turbulence kinetic energy budget and include the influence of rotation and stratification above the stable boundary layer. It is clear from their survey, that a large number of theoretical treatments have been offered in the past three decades which exceed the number of observational studies of the nocturnal boundary-layer. The Coriolis parameter is often considered as one of the scaling parameters in the similarity description of the stable boundary layer depth. Direct verification of the importance of the Coriolis parameter using data from a wide range of latitudes has not been carried out. Garratt (1982) compared a mid-latitude boundary layer with a low-latitude boundary layer and concluded that the differences between the two locations seemed to be due to differences in terrain rather than latitude. Nonetheless, observations of Ekman spirals have been observed in the stable nocturnal boundary layer (Van Ulden and Wieringa, 1996). Normally such spirals are difficult to isolate because of the influence of the nocturnal inertial oscillation (Section 4.4).

3.2. Very Stable

Turbulence in the very stable boundary layer (Figure 1) is weak and intermittent even near the surface, and perhaps layered at higher levels. Derbyshire (1990) argues that the turbulence may at least temporarily collapse due to strong net radiative cooling at the surface which demands a downward heat flux that cannot be supported by the turbulence. In the very stable boundary layer, the turbulence may be strongest at the top of the surface inversion layer (Mahrt, 1985) which may occur in shear on the underside of a low-level jet (Smedman, 1988). As a consequence, the depth of the very stable boundary layer may not be definable and models which assume a functional dependence of the exchange coefficients on z/h will probably not be successful, where h is the boundary-layer depth. Here, intermittency refers to *global intermittency* where turbulence is suppressed for periods which are long compared with the time scale of individual eddies (Mahrt, 1989). This contrasts with *local intermittency* which describes the variation of the fine-scale structure within individual large eddies (coherent structures).

Analyzing low-level aircraft data in the upper part of the nocturnal surface inversion, Ruscher and Mahrt (1989) found that some of the intermittent turbulence and most of the flux was associated with upward ejections of colder air apparently driven by local shear instability. The ejection motion spreads out horizontally leading to "two-dimensional" horizontal motions. The collision of such motions in narrow convergence zones contributed significantly to the averaged temperature variance but not to the averaged vertical flux.

Some studies suggest that the vertical profile of the heat flux is more curved in the very stable case corresponding to greater heat flux divergence in the lower part of the boundary layer (see, for example, Yamada, 1979). This heat flux profile could be forced by radiative flux divergence. Grant (1997) finds a tendency for greater curvature in the heat flux profile in the developing early evening nocturnal boundary layer. In principle, a wide variety of vertical distributions of the heat flux is possible in the very stable boundary layer.

3.3. Transition Between the Two Regimes

The above two-case division of the boundary layer is an oversimplification in that the stable boundary layer assumes a variety of forms (Mahrt *et al.* 1979; Stull, 1990; Kurzeja *et al.* 1991). For example, in the simple two-regime treatment above, the windy weakly stable boundary layer may contain a well-mixed layer or partially well-mixed layer between the stratified surface layer and overlying capping inversion, while the very stable case is more often characterized by profiles of potential temperature with negative curvature. However, Tjemkes and Duynkerke (1989) show cases where the potential temperature profile switches back and forth between these two regimes even though the surface heat flux was relatively time-independent.

Intermittent switching back and forth between turbulent and nonturbulent states has been historically posed in terms of a critical Richardson number and the feedback between turbulence fluxes and the mean profiles. Numerous observations have been interpreted in terms of interplay between generation of mean shear and reduction of shear by intermittent turbulence such that the Richardson number stays close to a critical value (Atlas *et al.* 1970; Roach, 1970; Townsend, 1976; Nieuwstadt, 1984; Kim and Mahrt, 1992; see also Derbyshire (1994) and references therein). The interplay between the intermittent turbulence and mean shear is not symmetric since generation of turbulence is thought to require much smaller Richardson numbers compared with the value required to maintain existing turbulence. In practice, exact values of the critical Richardson number are difficult to establish since the computed Richardson number generally increases with the thickness of the layer over which it is computed (Lyons *et al.* 1964; Kim and Mahrt, 1992) and turbulent sublayers may occur within layers of high Richardson number (Kunkel and Walters, 1982; Padman and Jones, 1985). Consequently, models based on a critical Richardson number might benefit by specifying the critical Richardson number to increase with grid size.

We unify the above discussion with previous sections by noting that the turbulence is more or less continuous in the weakly stable boundary layer while in the strongly stable boundary layer, fully developed turbulence only occurs intermittently where temporarily the boundary layer appears similar to the weakly stable case. The transition between the weakly stable and very stable cases is also marked by an increased relative importance of nonturbulent mesoscale motions which is discussed in more detail in Section 5.

4. Special Features of the Stable Boundary Layer

4.1. Enhanced Heterogeneity

It is unlikely that numerical and laboratory studies would intentionally include the influence of surface heterogeneity since understanding the stable boundary layer over homogeneous surfaces is far from complete. However, comparisons of numerical, theoretical, and laboratory studies with observations of atmospheric stable boundary layers must contend with the influence of surface heterogeneity on atmospheric stable boundary layers. Since vertical mixing in the very stable boundary layer is weak and characterized by small scales, small-scale heterogeneity may become important even though the influence of such heterogeneity in unstable heated boundary layers is eliminated by large eddies. On the other hand, mesoscale surface heterogeneity over flat surfaces is less likely to generate its own secondary circulation since larger scale vertical motion fields are preferentially inhibited by the stratification through pressure adjustments (Smith and Mahrt, 1981). Therefore the role of surface heterogeneity is mainly through modifying the local turbulence flux.

Derbyshire (1995a) emphasizes that the nocturnal boundary layer is slow to adjust and therefore easily influenced by surface heterogeneity and other variability. Because the mixing is smaller scale and weaker at night, small-scale obstacles and surface features are individually more likely to influence the surface layer compared with surface layers with weak stability or unstable stratification. Derbyshire (1995b) finds turbulence extending to larger Richardson numbers at a heterogeneous site compared with a homogeneous site which suggests that traditional formulations of the nocturnal boundary layer may underestimate turbulence with strong stratification over many real surfaces. Parker and Raman (1993) find multiple layer inversions and wind maxima and elevated layers of turbulence in nocturnal flow over complex terrain.

If the horizontal grid size of the model is large compared with turbulent scales and if the flow is not horizontally homogeneous, then similarity theory (Section 2) and the concept of a critical Richardson number do not apply to grid-averaged fluxes. Mahrt (1987) and Garratt (1992) argue that spatial variation of stability within an averaging area leads to turbulence at larger values of the Richardson number than predicted by applying similarity theory to spatially averaged variables. That is, even if the Richardson number based on spatially averaged variables is large, the Richardson number is still likely to be small at some locations within the averaging area. Therefore, the grid-averaged turbulent transport does not vanish with large Richardson number. These considerations imply that in numerical models with large grid size, the turbulence should extend to larger Richardson numbers than predicted by traditional similarity theory. Because of such spatial variability, Delage (1997) concludes that some turbulent mixing should be included in the model even for large Richardson numbers.

4.2. Turbulent Prandtl Number

The turbulent Prandtl number is sometimes assumed to be unity (Lacser and Arya, 1986; Tjemkes and Duynkerke, 1989) in which case $\varphi_\mathrm{h} = \varphi_\mathrm{m}$ in the surface layer and $K_\mathrm{h} = K_\mathrm{m}$ above the surface layer where K_h and K_m are the turbulent diffusivities for heat and momentum, respectively. The Prandtl number is thought to increase to values larger than one at larger Richardson numbers (Merrit and Rudinger, 1973; Hicks, 1976; Kondo *et al.* 1978; Wittich and Roth, 1984; Beljaars and Holtslag, 1991; Kim and Mahrt, 1992; Yagüe and Cano, 1994). Apparently, pressure fluctuations induced by turbulence and gravity waves lead to momentum flux without directly increasing the heat flux. For example, nonlinear gravity waves transport momentum but transfer little heat. Beljaars and Holtslag (1991) predict that the Prandtl number, $\varphi_\mathrm{h}/\varphi_\mathrm{m}$ increases as $(z/L)^{1/2}$. Consequently, the eddy Prandtl number is expected to be larger for the very stable case compared with the weakly stable case. However, exceptions occur and the Prandtl number for the Microfronts data remained near unity even for large stability (Howell and Sun, 1997).

4.3. Clear-Air Radiative Cooling

While stable stratification in the nocturnal boundary layer is induced by net radiative cooling at the surface, radiative flux divergence within the air may also be important. The importance of radiative flux divergence leading to clear-air radiative cooling was emphasized in Yamada (1979), Garratt and Brost (1981), and André and Mahrt (1982). Clear-air radiative cooling is thought to be most important in the very stable boundary layer. To first order, clear-air radiative flux divergence acts to cool warmer air and warm cooler air. This process leads to thickening of the surface inversion layer. Interaction between radiative effects and turbulent temperature fluctuations might increase the critical flux Richardson number (Townsend, 1958). This topic is beyond the scope of this survey and the reader is referred to Tjemkes and Duynkerke (1989) for further discussion.

4.4. Low Level Jet and Elevated Turbulence

Shear-generation of turbulence at the top of the surface inversion layer may be primarily due to formation of a low-level nocturnal jet (Figure 1) where turbulence is enhanced by shear on the underside of the jet (Smedman, 1988). This wind maximum can be generated by two main mechanisms: effects of sloped surfaces and inertial oscillations. Cooling over sloping terrain leads to a height-dependent pressure gradient force. Small-scale sloping terrain leads to nonhydrostatic downslope drainage flows which can be significant even over weak slopes if skies are clear and the large-scale flow is weak. Flows driven by slopes on scales greater than the order of 100 km become influenced by the Coriolis parameter (Lettau, 1990). A classification of different slope flows based on scale analysis of the basic equations is presented in Mahrt (1982).

As the second main mechanism, nocturnal low-level jets are driven by ageostrophic flow caused by daytime frictional effects in concert with collapse of the daytime boundary layer in late afternoon. This leads to the so-called inertial oscillation (Buajitta and Blackadar, 1957; Stull, 1990). The vertical resolution of large-scale models may be inadequate to resolve this transition as well as the vertical structure of the nocturnal boundary layer and overlying low level jet.

The initial formation of such a low-level jet can be viewed in terms of decoupling of the flow from the surface. The decoupled flow accelerates leading to elevated shear and generation of turbulence. Such turbulence was observed in a number of studies surveyed in Kim and Mahrt (1992) and also examined in Tjernström and Smedman (1993), Parker and Raman (1993), and Smedman *et al.* (1995). Shear associated with the low-level wind maximum may effectively generate turbulence just above the surface inversion layer in the overlying residual layer (Figure 1) where the stratification is weaker. The residual layer is the remnants of the previous days convectively mixed layer and is generally characterized by near neutral stratification. Eventually the elevated shear-driven turbulence generates sufficient turbulence that it diffuses to the surface in the form of intermittent turbulence. Coupling between the nocturnal boundary layer and the residual layer by intermittent turbulence is inferred in Mahrt *et al.* (1979) and Neu (1995).

The generation of the low-level jet by the inertial oscillation is complex. If momentum is well mixed during the day within the boundary layer above the surface layer and the geostrophic wind is independent of height, then the ageostrophic wind is also height-independent. The amplitude of the nocturnal inertial oscillation is proportional to the ageostrophic flow at the onset of the inertial oscillation. Therefore, without consideration of other factors, the collapse of the daytime boundary layer leads to an inertial oscillation whose amplitude is independent of height; that is, uniform acceleration of a deep layer with no well-defined local wind maximum. Height-dependent geostrophic wind enhances the height-dependent ageostrophic flow in the daytime since the baroclinic geostrophic wind varies with height while the momentum may be well mixed. For example, Arya and Wyngaard (1975) found that the actual shear in the mixed layer is considerably less than the geostrophic shear, enhancing the ageostrophic flow. Height-dependent ageostrophic flow may also be generated during the transition period between the daytime heated boundary layer and the nocturnal boundary layer (Mahrt, 1981; Grant, 1997). The boundary-layer depth collapses rapidly while the stress decreases more slowly with time leading to a temporary increase in the stress divergence in the lower levels. The transition period is difficult to model because the turbulence may not be in equilibrium with the rapidly changing mean flow (Grant, 1997).

5. Mesoscale Motions

Mesoscale motions include gravity waves, cold air drainage, and meandering motions which might propagate from outside the local domain and therefore not be included in numerical studies. Atmospheric stable

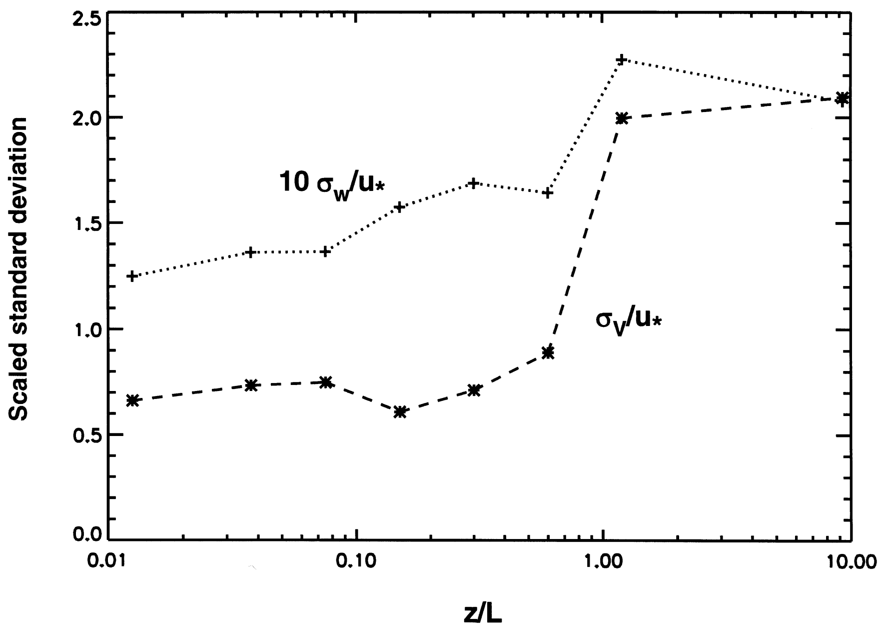

Figure 4. The standard deviation of the horizontal and vertical velocity fluctuations scaled by the surface friction velocity, as a function of stability for the Microfronts data. The standard deviation for the horizontal velocity fluctuations is the square root of the sum of variances for the u- and v-components.

boundary layers also frequently contain gravity waves (see Rao and Nappo (1998) and papers surveyed in Smedman (1991)) and other mesoscale variability of unknown origin. Such mesoscale motions complicate the comparison between observed and modeled statistics. These mesoscale motions become relatively more important for the very stable case, partly because they are more active and partly because the turbulence is weaker.

The mesoscale motions may also be locally generated in stably stratified flows by turbulence which decays into mainly horizontal modes sometimes referred to as meandering motions or two-dimensional turbulence (Kristensen *et al.* 1982; Lilly, 1983; Herring and Metais, 1989). Such meandering can be augmented by topographical effects or other causes of vertical directional shear (Grant, 1994). These layered motions randomly enhance the shear between layers which in turn intermittently regenerates local turbulence.

As a result of mesoscale motions and large eddies, Smedman (1988) finds that the standard deviation of the velocity fluctuations scaled by the surface friction velocity suddenly increase with increasing z/L for values greater than about 0.5. This increase is presumably due to the contribution of nonturbulent mesoscale motions to the variances. For the Microfronts data, the standard deviation of the velocity fluctuations scaled by the friction velocity increases substantially between z/L equal to 0.5 and 1.0 (Figure 4). The increased scaled standard deviations are due to the increased relative importance of the mesoscale motions. The mesoscale contribution might be reduced by using a smaller averaging scale to define the perturbation quantities for the very stable case, although such a procedure is somewhat arbitrary and inadvertently removes a small part of the turbulent flux. Mesoscale motions may also explain the decreased correlation between temperature and vertical motion with increasing stability observed by Smedman (1991).

Such mesoscale motions complicate comparisons between numerical simulations and stable atmospheric boundary layers since numerical domains do not naturally contain some of the above mesoscale motions. A simple comparison between the numerical simulations and atmospheric stable boundary layers can be formed in terms of variability of the horizontal flow. With substantial mesoscale variation of the wind vector, the speed of the time averaged wind vector is expected to be smaller than the time-average of the instantaneous wind speed due to flip-flop of the wind vector and cancellation in averaging the wind vector.

We therefore compute the ratio

$$CR \equiv \frac{[u]}{V}, \tag{11}$$

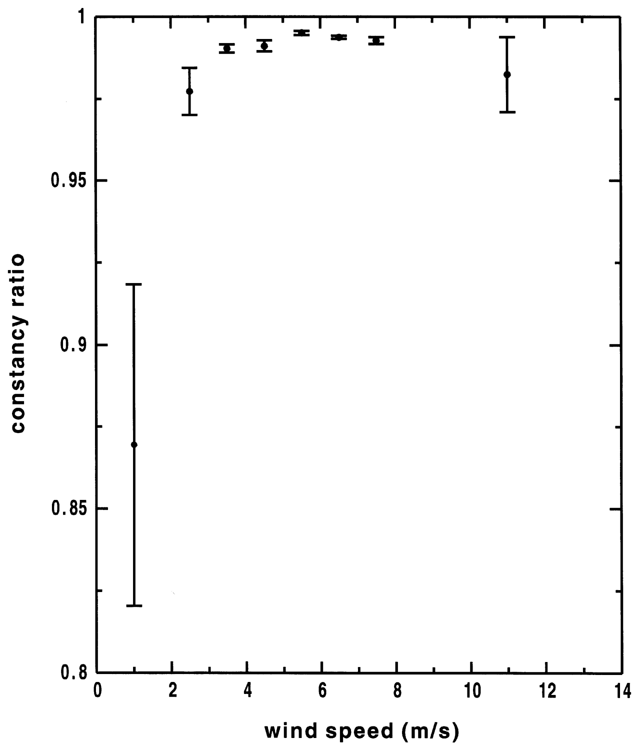

Figure 5. The constancy ratio as a function of wind speed for the Microfronts data.

where V is the average of the instantaneous wind speed and $[u]$ is the speed of the vector-averaged wind. This ratio is sometimes referred to as the constancy ratio. It represents the constancy or steadiness of the wind direction and is unity with constant wind direction. With strong continuous turbulence and absence of vigorous mesoscale motion, the ratio CR is close to unity, generally 0.98 or greater. That is, normal turbulence does not lead to large changes in wind direction. However with weak intermittent turbulence and mesoscale meandering of the wind vector, the constancy ratio will be smaller. Small CR should be an intrinsic feature of the very stable boundary layer and alerts the investigator that computed statistics will be sensitive to the averaging time. For nocturnal flow in the Microfronts experiment, the constancy ratio CR decreases with very weak winds to values less than 0.9 (Figure 5). The constancy ratio also decreases with increasing z/L although the relationship is not as systematic because the mesoscale contribution does not scale with z/L. Presumably CR would be larger in numerical models due to absence of some of the mesoscale activity.

As an additional complication, turbulence generated by mesoscale motions is not represented by the vector-averaged wind speed used in the bulk aerodynamic prediction of the surface fluxes (2) since such mesoscale motions reverse direction and are at least partly eliminated in the vector averaging process. This leads to new controversies in application of the bulk aerodynamic method discussed in Mahrt and Sun (1995) and references therein.

6. Conclusions and Summary of Special Modeling Problems

The above interpretive literature survey has organized the study of the stable boundary layer by considering two idealized prototype boundary layers: the weakly stable case and the very stable case. While this classification is partly supported by analysis of new eddy correlation data (Sections 3–5), any such classification is necessarily oversimplified.

Section 2 provides a self-contained approach for parametrizing surface fluxes in the stable boundary layer, briefly summarized in Section 2.5. Confident modeling of the very stable boundary layer seems tenuous due to suspected breakdown of current formulations of the surface fluxes.

1. Monin–Obukhov similarity theory for surface fluxes appears to underestimate turbulence in the very stable case (roughly $z/L > 1$) which may cause unrealistic surface cooling in models of the atmospheric boundary layer (Section 2). In numerical models, underestimation of the downward heat flux accelerates surface cooling and stabilization of the air adjacent to the surface. This further reduces the turbulence and downward mixing of warmer air. These feedback mechanisms can lead to unrealistically large surface cooling and total collapse of the turbulence.
2. In large-scale models, the thin very stable boundary layer may be resolved by only a couple of levels. With LES models, normally only the transporting eddies near the surface are unresolved and must be parametrized. However, in the interior of the very stable boundary layer, the transporting eddies may be locally generated by shear in thin layers and thus partly unresolved by the LES model. Data for testing subgrid parametrizations for the very stable case are not available.
3. The very thin surface layer may occur completely below the first model level z in which case current formulations of the surface fluxes are not valid. If z/h is not small compared with unity, where h is the boundary-layer top where the fluxes first vanish, then the flux at level z may be significantly smaller than the surface value. From another point of view, the flux–gradient relationship at level z depends on z/h as well as z/L and Monin–Obukhov similarity theory is not valid.

In addition to these difficulties, the stable atmospheric boundary layer includes physical effects which are not usually included in numerical models.

1. Inadequate resolution or omission of vertical divergence of the long-wave radiative flux which is thought to be important with strong stratification and augmented by strong vertical gradients of temperature, moisture, and other scalars.
2. Mesoscale motions such as gravity waves, meandering and cold air drainage can propagate from outside the domain of interest and can locally enhance the shear and shear-generation of turbulence.
3. Dominant shear-generation of turbulence at the top of the surface inversion layer causes the very stable boundary layer to lose its vertical integrity. When the main source of turbulence is elevated, definition of the nocturnal boundary layer becomes problematic and models which assume such a definition become invalid.
4. Low-level jets may involve large-scale flow features not fully recognized by the domain of the numerical model. The low-level jet can cause shear-generation of turbulence at or above the stable boundary layer but may also suppress large transporting eddies within the stable boundary layer. Then the height of the jet may become an additional length scale affecting the flux–gradient relationship even near the surface.

In conclusion, formulation of turbulence in the very stable boundary layer is uncertain and the stable boundary layer contains a number of physical influences not present in existing models. However, the very stable case is of considerable practical importance and even small future advances justify more work.

Acknowledgments

The author gratefully acknowledges many useful discussions with Jielun Sun, Anton Beljaars, and James Howell.

References

André, J.C., and Mahrt, L., 1982: The nocturnal surface inversion and influence of clear-air radiative cooling. *J. Atmos. Sci.*, **39**, 864–878.
Andrén, A., 1995: The structure of stably stratified atmospheric boundary layers: a large-eddy simulation study. *Quart. J. Roy. Met. Soc.*, **121**, 961–986.
Arya, S.P.S., 1972: The critical condition for the maintenance of turbulence in stratified flows. *Quart. J. Roy. Met. Soc.*, **98**, 264–273.

Arya, S.P.S., and Wyngaard, J.C., 1975: Effect of baroclinity on wind profiles and the geostrophic drag law for the convective planetary boundary layer. *J. Atmos. Sci.*, **32**, 766–778.

Atlas, D., Metcalf, J.I., Richter, J.H., and Gossard, E.E., 1970: The birth of "CAT" and microscale turbulence. *J. Atmos. Sci.*, **27**, 903–913.

Beljaars, A.C.M., and Holtslag, A.A.M., 1991: Flux parameterization over land surfaces for atmospheric models. *J. Appl. Meteor.*, **30**, 327–341.

Bergström, H., and Smedman, A., 1995: Stably stratified flow in the marine surface layer. *Boundary-Layer Meteorol.*, **72**, 239–265.

Brost, R.A., and Wyngaard, J.C., 1978: A model study of the stably stratified planetary boundary layer. *J. Atmos. Sci.*, **35**, 1427–1440.

Brown, A.R., Derbyshire, S.H., and Mason, P.J., 1994: Large-eddy simulation of stable atmospheric boundary layers with a revised stochastic subgrid model. *Quart. J. Roy. Met. Soc.*, **120**, 1485–1512.

Buajitti, K., and Blackadar, A.K., 1957: The theoretical studies of diurnal wind structure variation in the planetary boundary layer. *Quart. J. Roy. Met. Soc.*, **83**, 486–500.

Businger, J.A., Wyngaard, J.C., Izumi, Y., and Bradley, E.F., 1971: Flux-profile relationships in the atmospheric surface layer. *J. Atmos. Sci.*, **28**, 181–189.

Delage, Y., 1997: Parameterizing sub-grid scale vertical transport in atmospheric models under statically stable conditions. *Boundary-Layer Meteorol.*, **82**, 23–48.

Derbyshire, H., 1990: Nieuwstadt's stable boundary layer revisited. *Quart. J. Roy. Met. Soc.*, **116**, 127–158.

Derbyshire, H., 1994: A balanced approach to stable boundary layer dynamics. *J. Atmos. Sci.*, **51**, 3486–3504.

Derbyshire, H., 1995a: Stable boundary layers: observations, models and variability. Part I: Modelling and measurements. *Boundary-Layer Meteorol.*, **74**, 19–54.

Derbyshire, H., 1995b: Stable boundary layers: observations, models and variability Part II: Data analysis and averaging effects. *Boundary-Layer Meteorol.*, **75**, 1–24.

Dias, N.L., Brutsaert, W., and Wesley, M.L., 1995: Z-less stratification under stable conditions. *Boundary-Layer Meteorol.*, **75**, 175–187.

Garratt, J.R., 1982: Observations in the nocturnal boundary layer. *Boundary-Layer Meteorol.*, **22**, 21–48.

Garratt, J.R., 1992: *The Atmospheric Boundary Layer*. Cambridge University Press, Cambridge, 316 pp.

Garratt, J.R., and Brost, R.A., 1981: Radiative cooling effects within and above the nocturnal boundary layer. *J. Atmos. Sci.*, **38**, 2730–2746.

Grant, A.L.M., 1994: Wind profiles in the stable boundary layer, and the effect of low relief. *Quart. J. Roy. Met. Soc.*, **120**, 27–46.

Grant, A.L.M., 1997: An observational study of the evening transition boundary-layer. *Quart. J. Roy. Met. Soc.*, **123**, 657–677.

Haugen, D.A., Kaimal, J.C., and Bradley, E.F., 1971: An experimental study of Reynolds stress and heat flux in the atmospheric surface layer. *Quart. J. Roy. Met. Soc.*, **97**, 168–180.

Herring, J., and Métais, O., 1989: Numerical experiments in forced stably stratified turbulence. *J. Fluid Mech.*, **220**, 97–115.

Hicks, B.B., 1976: Wind profile relationships from "Wangara" experiments. *Quart. J. Roy. Met. Soc.*, **102**, 535–551.

Högström, U., 1988: Non-dimensional wind and temperature profiles in the atmospheric surface layer: a re-evaluation. *Boundary-Layer Meteorol.*, **42**, 55–78.

Högström, U., 1996: Review of some basic characteristics of the atmospheric surface layer. *Boundary-Layer Meteorol.*, **78**, 215–246.

Holtslag, A.A.M., 1984: Estimates of diabatic wind speed profiles from near-surface weather observations. *Boundary-Layer Meteorol.*, **29**, 225–250.

Holtslag, A.A.M., and De Bruin, H.A.R., 1988: Applied modeling of the nighttime surface energy balance over land. *J. Appl. Meteor.*, **27**, 689–704.

Howell, J., and Sun, J., 1997: Surface layer fluxes in stable conditions. Submitted to *Boundary-Layer Meteorol.*.

Kim, J., and Mahrt, L., 1992: Simple formulation of turbulent mixing in the stable free atmosphere and nocturnal boundary layer. *Tellus*, **44A**, 381–394.

Kondo, J., Kanechika, O., and Yasuda, N., 1978: Heat and momentum transfer under strong stability in the atmospheric surface layer. *J. Atmos. Sci.*, **35**, 1012–1021.

Kristensen, L., Jensen, N.O., and Peterson, E.L., 1982: Lateral dispersion of pollutants in a very stable atmosphere—the effect of the meandering. *Atmos. Environ.*, **15**, 837–844.

Kunkel, K.E., and Walters, D.L., 1982: Intermittent turbulence measurements of the temperature structure parameter under very stable conditions. *Boundary-Layer Meteorol.*, **22**, 49–60.

Kurzeja, R.J., Berman, S. and Weber, A.H., 1991: A climatological study of the nocturnal planetary boundary layer. *Boundary-Layer Meteorol.*, **54**, 105–128.

Lacser, A., and Arya, S.P.S., 1986: A numerical model study of the structure and similarity scaling of the nocturnal boundary layer (NBL). *Boundary-Layer Meteorol.*, **35**, 369–385.

Launiainen, J., 1995: Derivation of the relationship between the Obukhov stability parameter and the bulk Richardson number for flux-profile studies. *Boundary-Layer Meteorol.*, **76**, 165–179.

Lenschow, D.H., Li, X.S., Zhu, C.J., and Stankov, B.B., 1988a: The stably stratified boundary layer over the great plains. I. Mean and turbulence structure. *Boundary-Layer Meteorol.*, **42**, 95–121.

Lenschow, D.H., Zhang, S.F., and Stankov, B.B., 1988b: The stably stratified boundary layer over the great plains. II. Horizontal variations and spectra. *Boundary-Layer Meteorol.*, **42**, 123–135.

Lettau, H., 1990: The O'Niell experiment of 1953. *Boundary-Layer Meteorol.*, **50**, 1–9.

Lilly, D.K., 1983: Stratified turbulence and the mesoscale variability of the atmosphere. *J. Atmos. Sci.*, **40**, 749–761.

Louis, J.-F., 1979: A parametric model of vertical eddy fluxes in the atmosphere. *Boundary-Layer Meteorol.*, **17**, 187–202.

Lyons, R., Panofsky, H.A., and Wollaston, S., 1964: The critical richardson number and its implications for forecast problems. *J. Appl. Meteorol.*, **21**, 136–142.

Mahli, Y.S., 1995: The significance of the dual solutions for heat fluxes measured by the temperature fluctuation method in stable conditions. *Boundary-Layer Meteorol.*, **74**, 389–396.

Mahrt, L., 1981: The early evening boundary layer transition. *Quart. J. Roy. Met. Soc.*, **107**, 329–343.
Mahrt, L., 1982: Momentum balance of gravity flows. *J. Atmos. Sci.*, **39**, 2701–2711.
Mahrt, L., 1985: Vertical structure and turbulence in the very stable boundary layer. *J. Atmos. Sci.*, **42**, 2333–2349.
Mahrt, L., 1987: Grid-averaged surface fluxes. *Mon. Weather Rev.*, **115**, 1550–1560.
Mahrt, L., 1989: Intermittency of atmospheric turbulence. *J. Atmos. Sci.*, **46**, 79–95.
Mahrt, L., 1996: The bulk aerodynamic formulation over heterogeneous surfaces. *Boundary-Layer Meteorol.*, **78**, 87–119.
Mahrt, L., and Sun, J., 1995: Multiple velocity scales in the bulk aerodynamic relationship for spatially averaged fluxes, *Mon. Weather Rev.*, 123, 3032–3041.
Mahrt, L., Heald, R.C., Lenschow, D.H., Stankov, B.B., and Troen, I.B., 1979: An observational study of the structure of the nocturnal boundary layer. *Boundary-Layer Meteorol.*, **17**, 247–264.
Mahrt, L., Sun, J., MacPherson, J.I., Jensen, N.O., and Desjardins, R.L., 1997a: Formulation of the surface temperature for prediction of heat flux: application to BOREAS. *J. Geophy. Res.* **102**, 29,641–29,649.
Mahrt, L., Vickers, D., Sun, J., Højstrup, J., Hare, J., and Wilczak, J., 1997b: Heat flux in the coastal zone. to appear *Boundary-Layer Meteorol.*
Mason, P.J., and Derbyshire, S.H., 1990: Large eddy simulation of the stably-stratified boundary layer. *Boundary-Layer Meteorol.*, **53**, 371–400.
Merritt, G., and Rudinger, G., 1973: Thermal and momentum diffusivity measurements in a turbulent stratified flow. *AIAA J.*, **11**, 1465–1470.
Nappo, C.J., 1991: Sporadic breakdown of stability in the PBL over simple and complex terrain. *Boundary-Layer Meteorol.*, **54**, 69–87.
Neu, U., 1995: A parameterization of the nocturnal ozone reduction in the residual layer by vertical downward mixing during summer smog situations using sodar data. *Boundary-Layer Meteorol.*, **73**, 189–193.
Nieuwstadt, F.T.M., 1984: The turbulent structure of the stable, nocturnal boundary layer. *J. Atmos. Sci.*, **41**, 2202–2216.
Otte, M., and Wyngaard, J., 1996: A general framework for an "unmixed layer" PBL model. *J. Atmos. Sci.*, **53**, 2652–2670.
Padman, L., and Jones, I.S.F., 1985: Richardson number statistics in the seasonal thermocline. *J. Phys. Ocean.*, **15**, 844–854.
Parker, M.J., and Raman, S., 1993: A case study of the nocturnal boundary layer over a complex terrain. *Boundary-Layer Meteorol.*, **66**, 303–324.
Rao, K.S., and Nappo, C.J., 1998: Turbulence and dispersion in the stable planetary boundary layer. In *Advances in Fluid Mechanics Series: Dynamics of Atmospheric Flow*. Chapter 2. M.P. Singh and S. Raman, eds. Computational Mechanics Publications, Ashurst Lodge, Southampton. to appear.
Roach, W.T., 1970: On the influence of synoptic development on the production of high level turbulence. *Quart. J. Roy. Met. Soc.*, **96**, 413–429.
Ruscher, P., and Mahrt, L., 1989: Coherent structures in the very stable atmospheric boundary layer. *Boundary-Layer Meteorol.*, **47**, 41–54.
Sethuraman, S., and Brown, R.M., 1976: Validity of the log-linear profile relationship over a rough terrain during stable conditions. *Boundary-Layer Meteorol.*, **10**, 489–501.
Smedman, A.-S., 1988: Observations of a multi-level turbulence structure in a very stable atmospheric boundary layer. *Boundary-Layer Meteorol.*, **44**, 231–253.
Smedman, A.-S., 1991: Some turbulence characteristics in the stable atmospheric boundary layer. *J. Atmos. Sci.*, **48**, 856–868.
Smedman, A.-S., Tjernström, H., and Högström, U., 1993: Analysis of the turbulence structure of a marine low-level jet. *Boundary-Layer Meteorol.*, **66**, 105–126.
Smedman, A.-S., Bergström H., and Högström, U., 1995: Spectra, variances and length scales in a marine stable boundary layer dominated by a low level jet. *Boundary-Layer Meteorol.*, **76**, 211–232.
Smith, B., and Mahrt, L., 1981: A study of boundary layer pressure adjustments. *J. Atmos. Sci.*, **38**, 334–346.
Stull, R.B., 1990: *An Introduction to Boundary Layer Meteorology*. Kluwer, Boston, 666 pp.
Sun, J., 1997: Thermal and momentum roughness lengths. Submitted to *Boundary-Layer Meteorol.*.
Sun, J., and Mahrt, L. 1995: Determination of surface fluxes from the surface radiative temperature. *J. Atmos. Sci.*, **52**, 1096–1106
Sun, J., Massman, W., and Grantz, D.A., 1997: Aerodynamic variables in the bulk formula for turbulence fluxes. Submitted to *Boundary-Layer Meteorol.*.
Taylor, P.A., 1971: A note on the log-linear velocity profile in stable conditions. *Quart. J. Roy. Met. Soc.*, **97**, 326–329.
Tjemkes, S.A., and Duynkerke, P.G., 1989: The nocturnal boundary layer: Model calculations compared with observations. *J. Appl. Meteor.*, **28**, 161–175.
Tjernström, M., and Smedman, A.-S., 1993: The vertical structure of the coastal marine atmospheric boundary layer. *J. Geophys. Res.*, **98**, 4809–4826.
Townsend, A.A., 1958: The effects of radiative transfer on turbulent flow of a stratified fluid. *J. Fluid. Mech.*, **4**, 361–372.
Townsend, A.A., 1976: *The Structure of Turbulent Shear Flow*. Cambridge University Press, Cambridge, 429 pp.
Van Ulden, A.P., and Wieringa, J., 1996: Atmospheric boundary-layer research at Cabauw. *Boundary-Layer Meteorol.*, **78**, 34–69.
Vogelezang, D.H.P., and Holtslag, A.A.M., 1996: Evaluation and model impacts of alternative boundary-layer height formulations. *Boundary-Layer Meteorol.*, **81**, 245–269.
Webb, E.K., 1970: Profile relationships: the log-linear range, and extension to strong stability. *Quart. J. Roy. Met. Soc.*, **96**, 67–90.
Wittich, K.-P., and Roth, R., 1984: A case study of nocturnal wind and temperature profiles over the inhomogeneous terrain of Northern Germany with some considerations of turbulent fluxes. *Boundary-Layer Meteorol.*, **28**, 169–186.
Wyngaard, J.C., 1973: On surface-layer turbulence. In *Proc. Workshop on Micrometeorology*, D.A. Haugen, ed., Amer. Meteorol. Soc., Boston, pp. 101–149.
Yaglom, A.M., 1977: Comments on wind and temperature flux-profile relationships. *Boundary-Layer Meteorol.*, **11**, 89–102.

Yagüe, C., and Cano, J., 1994: The influence of stratification on heat and momentum turbulent transfer in Antarctica. *Boundary-Layer Meteorol.*, **69**, 123–136.

Yamada, T., 1979: Prediction of the nocturnal surface inversion height. *J. Appl. Meteor.*, **18**, 526–531.

Zilitinkevich, S.S., and Chalikov, D.V., 1968: On the determination of the universal wind and temperature profiles in the surface layer of the atmosphere. *Izv. Acad. Sci. USSR., Atmos. Oceanic Phys.*, **4**, 915–929.

Zilitinkevich, S.S., and Mironov, D., 1996: A multi-limit formulation for the equilibrium depth of a stably stratified boundary layer. *Boundary-Layer Meteorol.*, **81**, 325–351.